SCIENTIFIC REPORTS

OPEN

Complex multifractal nature in *Mycobacterium tuberculosis* genome

Saurav Mandal[1], Tanmoy Roychowdhury[2], Keilash Chirom[1], Alok Bhattacharya[1,3] & R. K. Brojen Singh[1]

The mutifractal and long range correlation (*C(r)*) properties of strings, such as nucleotide sequence can be a useful parameter for identification of underlying patterns and variations. In this study *C(r)* and multifractal singularity function $f(\alpha)$ have been used to study variations in the genomes of a pathogenic bacteria *Mycobacterium tuberculosis*. Genomic sequences of *M. tuberculosis* isolates displayed significant variations in *C(r)* and $f(\alpha)$ reflecting inherent differences in sequences among isolates. *M. tuberculosis* isolates can be categorised into different subgroups based on sensitivity to drugs, these are DS (drug sensitive isolates), MDR (multi-drug resistant isolates) and XDR (extremely drug resistant isolates). *C(r)* follows significantly different scaling rules in different subgroups of isolates, but all the isolates follow one parameter scaling law. The richness in complexity of each subgroup can be quantified by the measures of multifractal parameters displaying a pattern in which XDR isolates have highest value and lowest for drug sensitive isolates. Therefore *C(r)* and multifractal functions can be useful parameters for analysis of genomic sequences.

Genomic alteration through a number of mechanisms (mutation, substitution, duplication, deletion, insertion, and selection etc.) in combination with natural selection provides a basis of evolution. However, evolution does maintain some conserved features that are characteristics of the organisms. The generic features of these conserved properties can be characterized by the scaling laws[1,2] emerging from one dimensional genome sequence. These laws are preserved and inherited in the complex evolutionary process. Scaling law of an observable $y(x)$, which manifests preserved properties in the system, can be quantified through scaling functions $F[x, y(x)]$ and $\Gamma[y(x)]$[3,4], and follows self-affine process for any scale factor c[5], given by

$$y(x) = F[x, y(x)]; \frac{dlny(x)}{dlnx} = \Gamma[y(x)]; y(x) = Ax^{\gamma}: \frac{y(cx)}{y(x)} = c^{D}, \forall t, 0 < c < 1 \tag{1}$$

where, A is a constant, and D is the self-similarity dimension of the self-affine process. If this $y(x)$ involves a few number of fractal rules then it obeys Mandelbrot's classical multifractal rules for self-affine process[6],

$$\frac{y(cx)}{y(x)} = U(c); U(c_1 c_2 ... c_n) = U_1(c_1) U_2(c_2) ... U_n(c_n): U_{\kappa}(c_{\kappa}) \sim c_{\kappa}^{D_{\kappa}}, \forall t, 0 < c, c_1, c_2 ..., c_n < 1 \tag{2}$$

One of the conserved properties is genomic correlation function $C(r)$ of the DNA sequence which follows the fractal rule[7]: $C(r) \sim r^{-\varepsilon}$, with $D = -\varepsilon$. The value of D is different for different biological processes; for genome length distribution in unicellular organisms $D = 1/4$[8], for distribution of RNA concentration $D = 1/4$[8], for metabolic process $D = -3/4$[9], for heart rate $D = 1/4$[8], for life span of the organism $D = -1/4$[9], for the distribution of radii of aortas and tree trunks $D = -3/8$[9].

Multifractal properties of DNA can be characterized by long range correlation maintained in the whole genome[7], and pseudorandom distribution of nucleotides[10] following an overall probability distribution. These can be represented as a DNA walk in two dimensional space[10,11]. Even though multifractal detrended fluctuations analysis (MF-DFA) technique is particularly important for a varity of time series data analysis[12], such as sunspot

[1]School of Computational and Integrative Sciences, Jawaharlal Nehru University, New Delhi-110067, India. [2]Department of Health Sciences Research, Mayo Clinic, Rochester, MN, USA. [3]School of Life Sciences, Jawaharlal Nehru University, New Delhi-110067, India. Correspondence and requests for materials should be addressed to R.K.B.S. (email: brojen@jnu.ac.in)

time series[13], stock exchange rate time series data[14], complicated earthquake data[15], social and religious dynamics[16], traffic flow time series[17], energy stocks data[18], brain EEG data[19], human DNA sequence[20], the application of this technique for analysis of Next Generation Sequencing (NGS) data of organisms for extraction of useful information may be challenging.

Mycobacterium tuberculosis is a slow growing pathogen that causes Tuberculosis (TB) and it is one of the major public health challange particularly among lower and middle income countries[21,22]. Drug resistance is one of the major concerns for treatment of patients with this disease and occurrence of extreme drug resistance (XDR) may make the scenario even worse. Drug resistant genes such as *rpoB*[23,24], *inhA*[25], *katG*[26], *gyrA*[27], *ahpC*[28], *embB*[29], *pncA*[30] have been experimentally identified. Different isolates of this bacterium have been classified into various lineages using sequence features and these lineages show correlation with geographical location. Recent genomic studies have found relationship between sequence differences among different isolates (represented by single nucleotide polymorphisms or SNPs and different repetitive sequences) and lineages[31,32]. Drug resistance isolates can be classified into different categories depending upon level of resistance. Multi Drug Resistance isolates (MDR) are insensitive to a few drugs whereas XDR isolates are resistant to a number of drugs. In recent times there has been an increase in the number of patients infected with both MDR-TB and XDR-TB, over 480,000 people developed multidrug-resistance TB in 2014[22]. India, the Russian Federation and the Peoples Republic of China reported half of the cases of MDR-TB and an estimate of around 9.7% of MDR-TB cases are likely to be also XDR-TB[22]. Changes in genomic sequences are not distributed randomly, some regions (hotspots) display high level of variations whereas a few others are highly conserved (coldspots)[33]. In our analysis we considered a few genes that display significant variations among drug resistant strains and are thought to be involved in drug resistance, such as *rpoB*, *phoP* and *phoR*. Sequences from some of these genes that map to the same strand of the genome from different *M. tuberculosis* isolates were concatenated to make a single sequence for multifractal analysis[34]. These sequences were obtained from NGS datasets of available isolates[35,36]. The results showed that C(r) and Multifractal analysis can be useful parameters for classification of drug resistant isolates.

Results and Discussion

Theory of multifractality in genome evolution.
Genome alterations in *M. tuberculosis*, due to various internal and external factors (e.g. continuous encounter with drugs and immune response of the host), is associated with sequence changes that involve substitution with different nucleotide, insertion and deletion, expansion of repeats, recombination and activity of transposable elements. NGS has allowed rapid and inexpensive method of getting complete nucleotide sequence, however the sequences come out as short reads. The nucleotide variation in these isloates are found to be not uniform, and large variations occur in few regions (called *hotspots*)[37] and few genes only[23–30]. One dimensional *DNA walk*[38] is generated from the genome sequence $\{x_i; i = 1, 2, …, N\}$ of each isloate (Fig. 1, Fig. 2 uppermost panels), where $x_i = +1$ for purine (A and G), and $x_i = -1$ for pyrimidine (C and T)[10]. Major unaltered portion of the genome of each isolate maintains same long range correlation $C(r) \propto r^{-\beta}$ as reference genome with observed root mean square fluctuations of *DNA walk*, $W(r) \propto r^{\gamma}$, where, $\gamma = 1/2$ for long range ($r \to large$), and short range ($r \to 0$); and $\gamma \neq 1/2$ for infinite range $r \to \infty$[38] exhibiting multifractal nature[5,6,12]. The specific genomic portions of each isolate (concatenated similar drug resistant genes), where significant amount of alterations are exhibited as compared to reference genome, show long range correlations $C(r) \propto r^{-\varepsilon}$[7] (Fig. 1, Fig. 2 middle panels), with fluctuation function $F_q(s)$ of order q (see Methods) obeying power law, $F_q(s) \propto s^{H_q}$ (Fig. 1, Fig. 2 lower most panels), where, H_q is generalized Hurst exponent[12], showing indication of multifractal nature in the genes.

Since the differences in the phenotypic and genotypic characters of each and every isolates from the reference *M. tuberculosis* genome(*H37Rv*) are due to the variations in the sequences of few hotspots and genes, local scaling properties of *highly polymorphic regions(HPR)* which are concatenated similar drug resistant genes may provide the characteristics of the perturbation induced in the reference genome and gets adapted to it. Consider a *DNA walk* of a *HPR* which can be divided into m segments $\{u_i; i = 1, 2, …, N\}$. Then the probability that the ith segment having length scale r can have N_i observations for large N, which is given by $\Lambda_i(r) = \lim_{N \to \infty} \frac{N_i}{N}$, holds the following power law in the limit $r \to 0$[39],

$$\Lambda_i(r) \sim r^\alpha \tag{3}$$

where, α is Holder or singularity exponent[40] which serves as the measure of crowding index in *HPR*. If $N(r, \alpha)$ is the number of segments in which Λ_i has singularity strength between α and $\alpha + \Delta\alpha$, then $N(r, \alpha)$ obeys[39],

$$N(r, \alpha) \sim r^{-f(\alpha)} \tag{4}$$

where, $f(\alpha)$ is the singularity function which can be related to the observable properties of a certain experimental measure. $f(\alpha)$ can also be known as fractal dimension of the set of segments with singularity strength α. It can be related to another important generalized dimension D_q of order q which can be defined by[41,42],

$$D_q = \lim_{r \to 0} \frac{1}{q-1} \frac{\ln[\sum_i \Lambda_i^q(r)]}{\ln(r)} \tag{5}$$

Different values of D_q characterize distribution in the segments with different degree of clustering in it. For non-stationary *DNA walk*, $D = \lim_{q \to +\infty} D_q$ and $D = \lim_{q \to -\infty} D_q$ corresponds to fractal dimensions of most and least populated segments respectively. D_q can be related to $f(\alpha)$ by employing Legendre transformation to its expression, and can be obtained as[39,43,44],
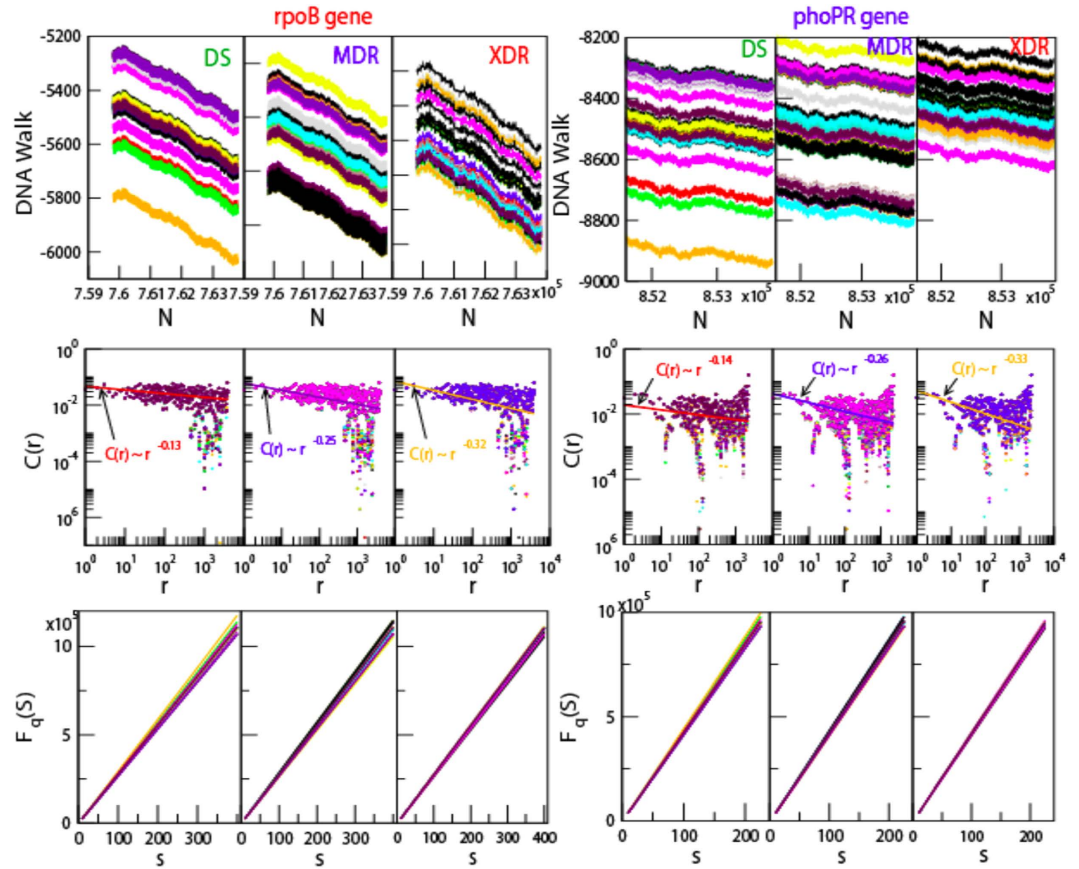
Figure 1. Multifractal and correlation function behaviors of *rpoB* gene (sequence positions: 759807–763325), *phoP* and *phoR* gene combined together(sequence positions: 851608 to 853853) in *M. tuberculosis* genome. (**a**) DNA walks of forty isloates each of DS, MDR and XDR of *M. tuberculosis* (panels of uppermost row). (**b**) Corresponding plots of correlation functions (*C(r)* versus *r*) of the three types of isloates (panels of middle row). Straight lines are power law fits on the data (for *rpoB* gene: DS: $C(r) \sim r^{-0.13}$; MDR: $C(r) \sim r^{-0.25}$; XDR: $C(r) \sim r^{-0.32}$ and for *phoPR* gene complex: DS: $C(r) \sim r^{-0.14}$; MDR: $C(r) \sim r^{-0.26}$; XDR: $C(r) \sim r^{-0.33}$). (c) Plots of fluctuation function ($F_q(s)$) with respect to *s* for the corresponding three types of *M. tuberculosis* isloates showing power law nature (panels of lowermost or third row).

$$f(\alpha) = q\alpha - \tau(q); \ \tau(q) = (q - 1)D_q = qH_q - 1; \ \alpha = \frac{d\tau}{dq} = H_q + q\frac{dH_q}{dq} \tag{6}$$

where, τ is another classical multifractal scaling exponent[43,44].

For *HPR*, $f(\alpha)$ is singularity spectrum with $\Delta\alpha = \alpha_{max} - \alpha_{min} = H_{-\infty} - H_{\infty}$ as width of the singularity spectrum, which is a quantitative multifractal strength. Further, $f(\alpha) \to 0$, if $\alpha \to H_{\infty}$ and $\alpha \to H_{-\infty}$[45,46]. If the *DNA walk* is monofractal, H_q is independent of q, and so from (6), $\alpha = constant$, $\tau(q)$ is linear function of q, and $f(\alpha)$ is constant with α.

The calculated $f(\alpha)$ as a function of α for forty isolates each of DS, MDR and XDR of *M. tuberculosis* shows different maxima values of $f(\alpha)$, but shows similar structural behavior (Figs 3 and 4 upper panels). The average $f(\alpha)$ along α shows significant difference in three different type of isolates (DS, MDR and XDR), except average $f(\alpha)$ values of DS and MDR isolates are approximately overlapping(Figs 3 and 4 the panels in the first and third rows). The scaled behavior of $f(\alpha)$ with α for each type of isolate shows approximately similar nature (Figs 3 and 4 insets in the panels of first and third rows).

The complexity of the *DNA walk* can be measured by expanding the singularity function $f(\alpha)$ around α_0, with $f(\alpha_0) \to f_{max}$ (maximum value of $f(\alpha)$), by Taylor's series,

$$f(\alpha) = f[\alpha_0 + (\alpha - \alpha_0)] = \sum_{i=0}^{\omega} a_i(\alpha - \alpha_o)^i; \ a_i = \frac{1}{i!}\frac{d^i f(\alpha)}{d\alpha^i}\bigg|_{\alpha \to \alpha_0} \to constant \tag{7}$$

where, ω is the degree of the truncated polynomial. Then fitting the $f(\alpha)$ data of *DNA walk* with the polynomial (7), the following multifractal parameters can be calculated: α_o, α_{min}, α_{max}, and $\Delta\alpha = \alpha_{max} - \alpha_{min}$. The symmetry of each singularity spectrum can be quantified by defining a skew parameter,
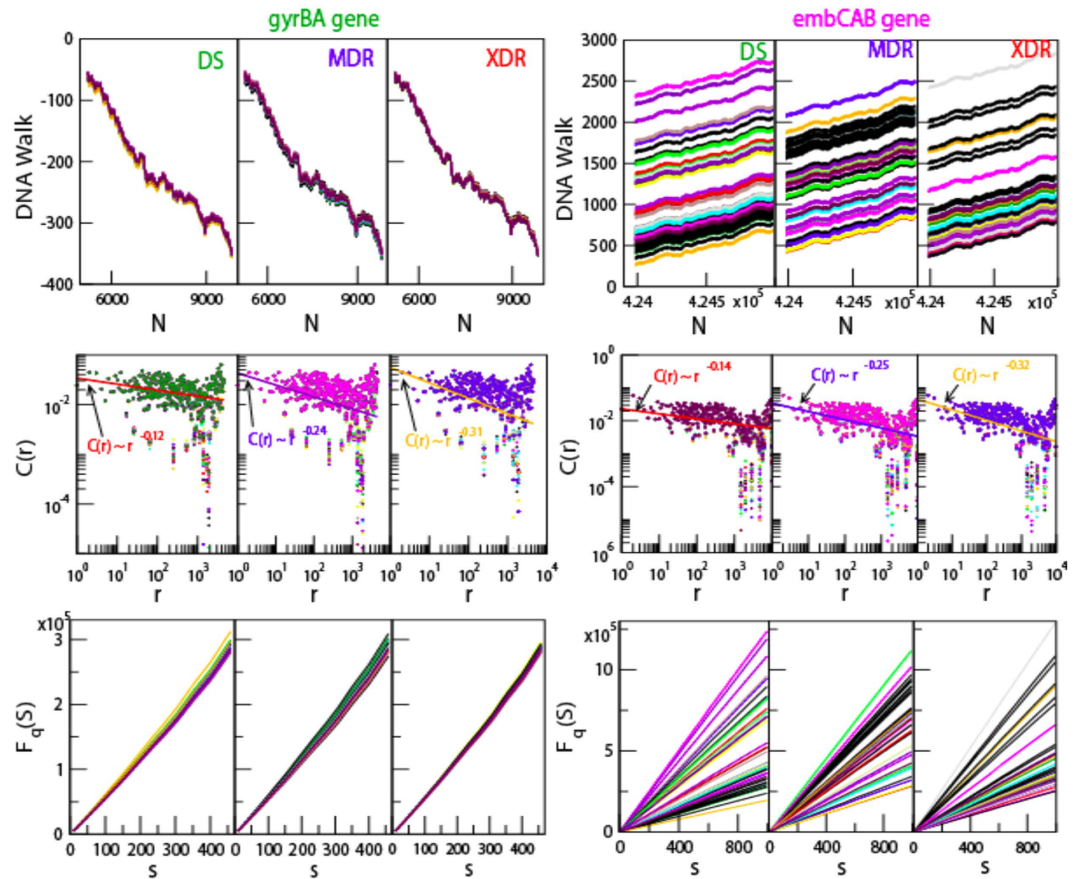
Figure 2. Multifractal and correlation function behaviors of *gyrB* gene and *gyrA* gene concatenated together (sequence positions: 5240–9810) and *embC, embA* and *embB* gene concatenated together with sequence position from 4239863 to 4249810 in *M. tuberculosis* genome. (**a**) DNA walks of forty isloates each of DS, MDR and XDR of *M. tuberculosis* (panels of uppermost row). (**b**) Corresponding plots of correlation functions ($C(r)$ versus r) of the three types of isloates (panels of middle row). Straight lines are power law fits on the data (for *gyrBA*: DS: $C(r) \sim r^{-0.12}$; MDR: $C(r) \sim r^{-0.24}$; XDR: $C(r) \sim r^{-0.31}$ and for *embCAB*: DS: $C(r) \sim r^{-0.14}$; MDR: $C(r) \sim r^{-0.25}$; XDR: $C(r) \sim r^{-0.32}$). (**c**) Plots of fluctuation function ($F_q(s)$) with respect to s for the corresponding three types of *M. tuberculosis* isloates showing power law nature (panels of lowermost or third row).

$$\chi = \frac{\alpha_{max} - \alpha_0}{\alpha_{min} - \alpha_0}; \begin{cases} \text{Right-skewedshape, if} & \chi > 1 \\ \text{Left-skewedshape, if} & \chi < 1 \\ \text{symmetric, if} & \chi = 1 \end{cases} \tag{8}$$

Small value of α_0 correspond to more regular struture in the *HPR*[14]. $\Delta\alpha \rightarrow large$ indicates stronger multifractality due to richness in structure of the genome. $\chi > 1$ reveals the dominance of scaling by small fluctuations and higher Hurst exponents, and indicating the presence of fine structure process in the genome. However, $\chi < 1$ indicates the dominance of scaling by large fluctuations of singular spectrum and relatively small Hurst exponents showing correlation in the signal corresponding to absence of fine structure process in the signal. Richness in complexity in the *HPR* corresponds to large value of α_0, wide range of $\Delta\alpha$, and $\chi > 1$[14,47].

The nature of α_0 for DS and MDR type of isolates are closely similar to each other. This similar behavior is due to the similarity in sequence variation in these two types of isolates, which exhibits similar multifractal behaviors (Figs 3 and 4 extreme left panels in second and fourth rows). The average values of α_0 for the four genes in the three isolates DS, MDR and XDR are found to be different but follow similar behavior (Figs 3 and 4 fourth panels in second and fourth rows). Similar properties of these two types of isolates are also exhibited in the nature of $\Delta\alpha$ (Figs 3 and 4 second leftmost and fifth panels in second and fourth rows), and in the behaviour of χ (Figs 3 and 4 third leftmost and sixth panels in the second and fourth rows). Comparatively large values of $\Delta\alpha$ and χ values in XDR as compared to those of DS and MDR indicates significant richness in multifractality in XDR. Further, since $\chi < 1$ (slightly left skewed) for all the three types of isolates, the sequence alteration in the *HPR* is due to genome evolution in *M. tuberculosis*. This induces large fluctuation in the singular function and small in Hurst exponents driving more correlation in the signal and causing destruction of fine structure process in the signal. Since the
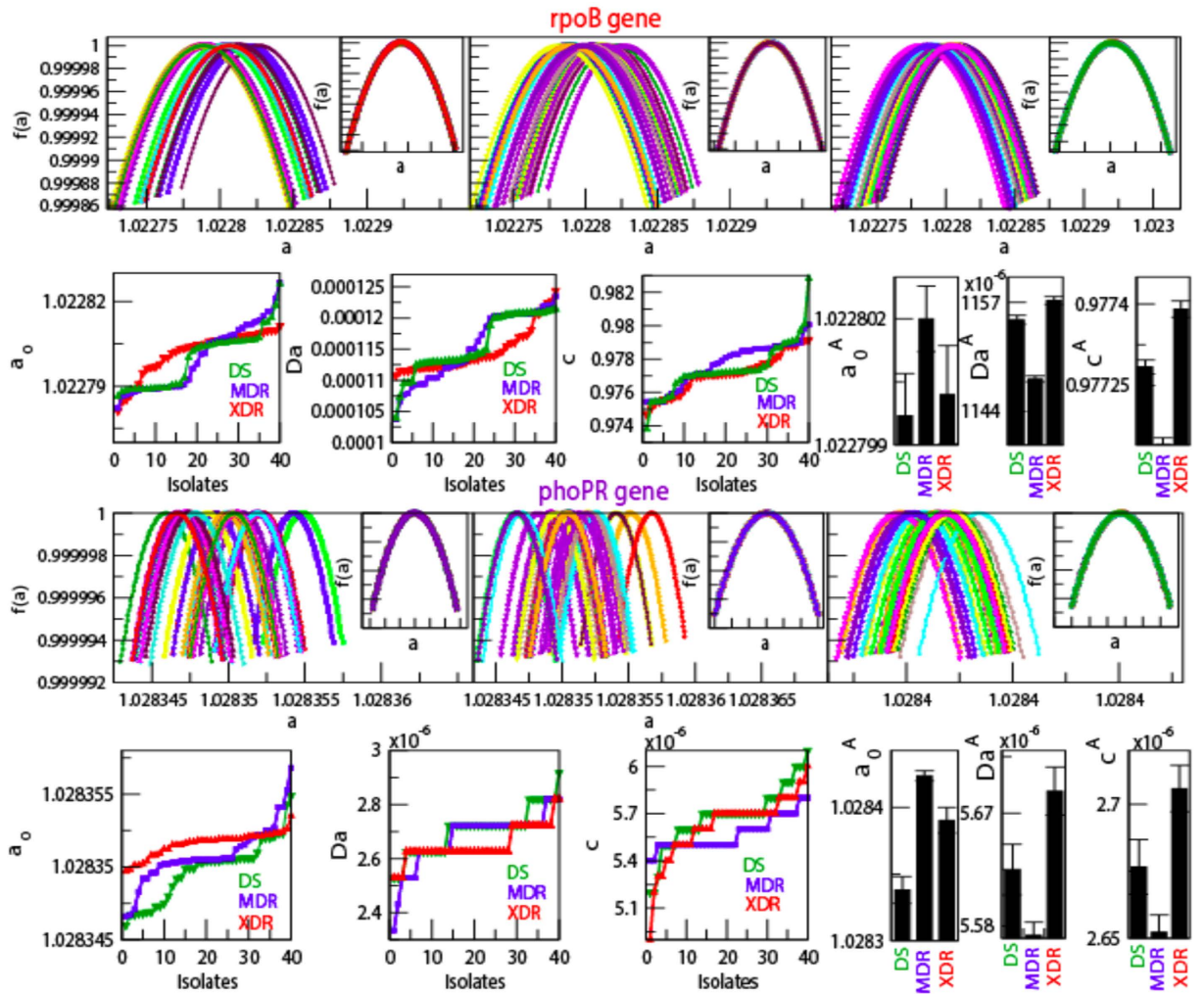
Figure 3. Singularity spectrum of *rpoB* gene and *phoPR* gene complex of *M. tuberculosis* isolates (forty) of each DS, MDR and XDR. (**a**) Plots of singularity function $f(\alpha)$ of the three types of isolates with respect to α (panels of first row) and their Scaling of $f(\alpha)$ by choosing $\alpha_c = 1.02275$ using interpolation showing self-affine process of the isolates (inside box). (**b**) Properties of multifractal spectral parameters: behaviors of α_0, $\Delta\alpha$ and χ as a function of isolates (colors show types of isolates).

changes in these parameters are small, these sensitive parameters (α_0, $\Delta\alpha$ and χ) can capture small changes in the multifractal nature due to few sequence alterations in the *HPR* significantly.

SNP based sequences of *M. tuberculosis* isolates show multifractal nature.

The whole genome of each isolate is mapped to the reference genome, and the SNP are arranged in a string without changing their positions but removing the nucleotides in between any pair of SNPs in the genome. The constructed *SNP based sequences* have varied lengths depending on the isolates, ranging from 432 bp to 4000 bp in length. We look at the multifractal properties of these *SNP based sequences* to understand fundamental mechanism of genome evolution (See Table1 in Supplementary file).

DNA walks of these *SNP based sequences* exhibit different behaviors for the three different classes DS, MDR and XDR (Fig. 5 uppermost row, first three panels). The one dimensional correlation function $C(r)$ of these SNP based sequences is calculated using the procedure of Messer *et al.*[48] (see Methods). The calculated $C(r)$s of all forty isolates of each class are plotted together (Fig. 5 second row), and the data as a whole follows power law,

$$C_k(r) \sim r^{-\theta_k}; \begin{bmatrix} \theta_s \\ \theta_m \\ \theta_x \end{bmatrix} \rightarrow \begin{bmatrix} 0.23 \\ 0.35 \\ 0.43 \end{bmatrix} \qquad (9)$$

where, k indicates isolate types: $k \rightarrow s, m, x$ for DS, MDR and XDR respectively. The best fitted curve on the data with power law (9) gives different values of θ_k for different class. This power law behavior of $C(r)$ versus r for individual as well as groups of isolates (DS, MDR, and XDR) are verified following a standard statistical fitting
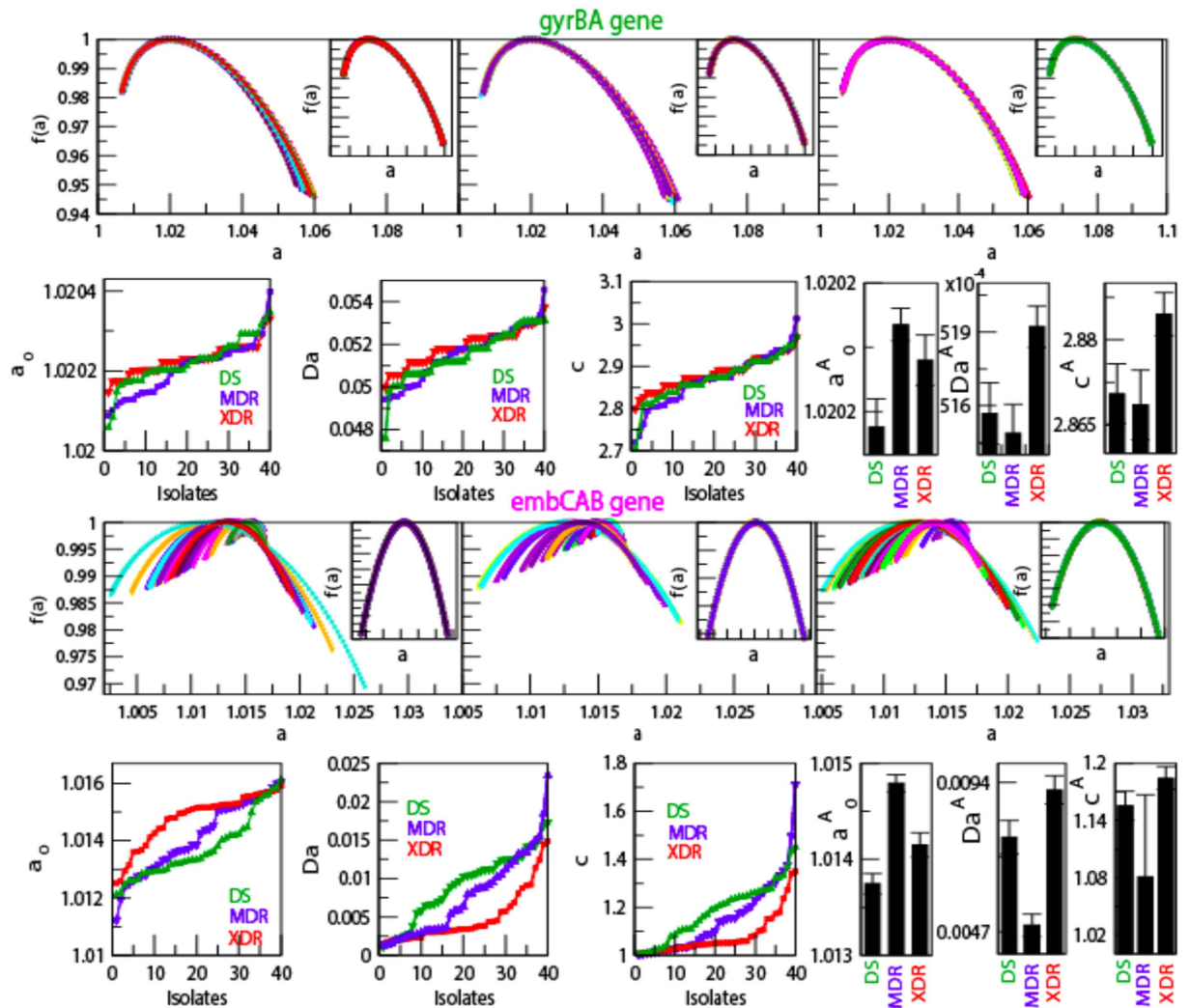
Figure 4. Singularity spectrum of *gyrBA* gene complex(sequence position: 5240 to 9810) and *embCAB* gene complex(sequence position: 4239863 to 4249810) of *M. tuberculosis* isolates (forty) of each DS, MDR and XDR. (a) Plots of singularity function $f(\alpha)$ of the three types of isolates with respect to α (panels of first row) and their Scaling of $f(\alpha)$ by choosing $\alpha_c = 1.02275$ using interpolation showing self-affine process of the isolates (inside box). **(b)** Properties of multifractal spectral parameters: behaviors of α_0, $\Delta\alpha$ and χ as a function of isolates (colors show types of isolates).

procedure[49], and found that the p-values (statistical level of significance) of each fitting on the dataset is found to be more than predicted critical value ($p-value > 0.1$). This change in the θ_k could be due to changes in SNPs in the *SNP based sequences* of different types of isolates of *M. tuberculosis*.

The calculated singularity spectra $f(\alpha)$ as a function of α for various isolates in different types of isolates exhibit different structures (Fig. 5 third row). Calculated α_0 for different types of isolates (Fig. 5 Lowermost row extreme left panel) shows comparatively large values as compared to those of *HPR*, indicating the possibility of associating complex multifractal features in the *SNP based sequences*. The range of singularity spectra $\Delta\alpha$ for the types of isolates are also significantly large showing wide range of multifractal nature (Fig. 5 Lowermost row third plot). The shape of singularity spectra of all the isolates of different classes are found to be right skewed ($\chi > 1$) which are the signature of the existence of fine structures in the *SNP based sequences* due to rich complex multifractal behavior. Further, the values of α_0, $\Delta\alpha$ and χ for XDR *SNP based sequences* are found to be approximately larger than the other types showing richer possession of multifractal properties.

Scaling in genomic correlation function. The changes in *HPR* and *SNP based sequences* in different isolates of DS, MDR and XDR are due to selection of *M. tuberculosis* that are undergone sequence changes allowing resistance to drugs in the course of time[50]. This selection process is the one that allows only some isolates with altered genotypic and phenotypic properties leading to genome evolution[51,52]. These changes are species specific and affected very much by many factors including host immune systems and climatic conditions[53]. The spatio-temporal alterations in sequences in the isolates due to sequence alterations (mutations, deletions, duplications, insertions, substitutions, selections) can be nicely modeled using the proposed sequence evolution
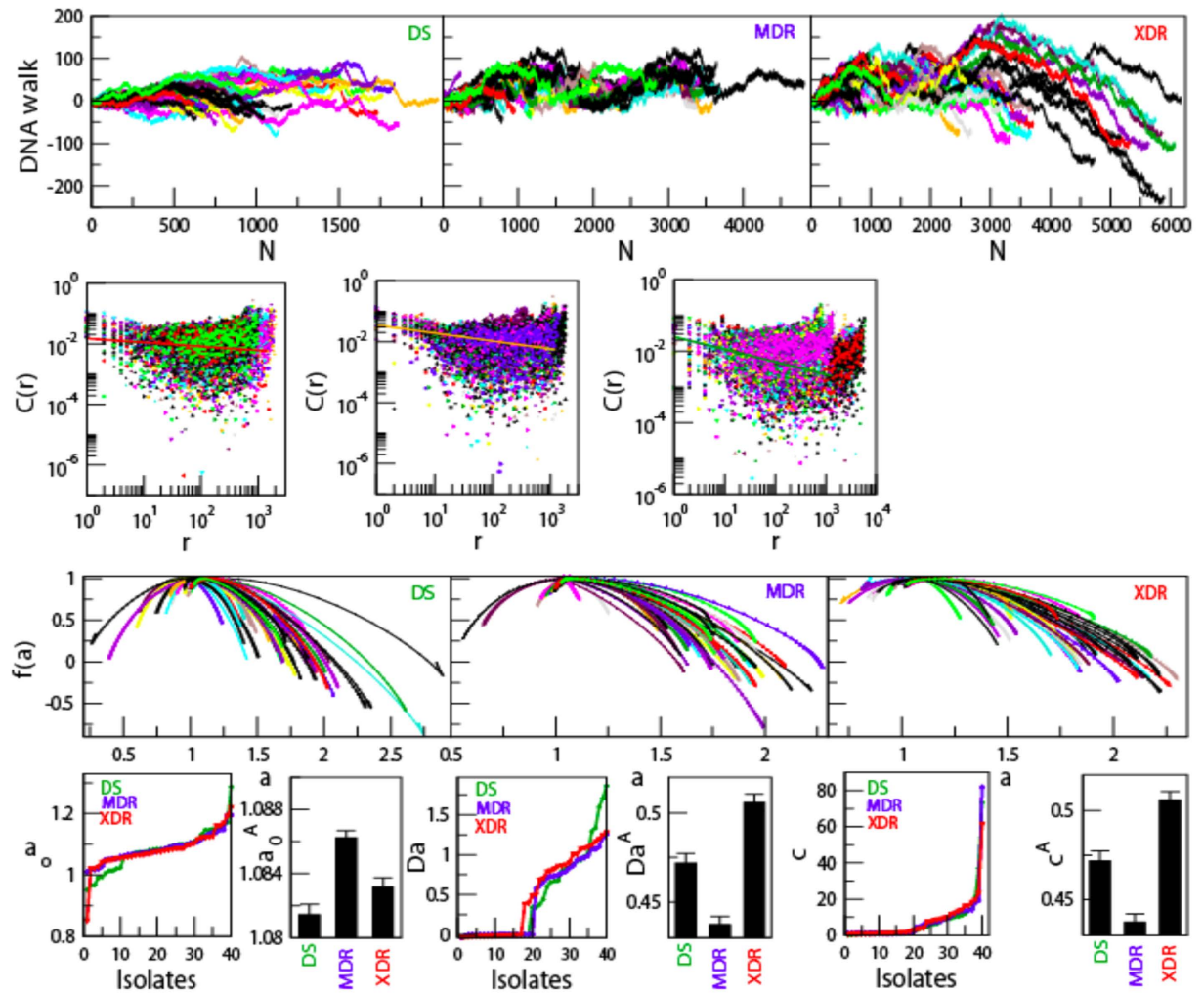
Figure 5. Multifractal and correlation function behaviors of all SNPs (*SNPs based Sequences*) within a genome of forty isolates each from DS, MDR and XDR. (**a**) DNA walks of forty isolates each of DS, MDR and XDR of *M. tuberculosis* (the first three panels of uppermost row). (**b**) Corresponding plots of correlation functions (C(r) versus r) of the three types of isolates (first three panels of second row). Straight lines are power law fits on the data (for DS: $C(r) \sim r^{-0.23}$; MDR: $C(r) \sim r^{-0.35}$; XDR: $C(r) \sim r^{-0.43}$). (**c**) Plots of singularity function $f(\alpha)$ of the three types of isolates with respect to α (first three panels of third row). (**d**) Properties of multifractal spectral parameters: behaviors of α_0, $\Delta\alpha$ and χ as a function of isolates (colors show types of isolates) in the bottom row.

model[7,54], and some of the observables can be characterized by the dynamics of position dependent one dimensional sequence compositional correlation, $C(r) = <s_i s_{i+r}>(t)$. Defining $C(r) = P_E(r,t) - P_O(r,t)$, where, P_E and P_E are joint probabilities of finding any two symbols equal and opposite in sign and following their own Master equations, one can arrive at the following evolutionary dynamics of $C(r)$ for $r \gg 1$ (long range correlation),

$$\frac{\partial C(r,t)}{\partial t} = -AC(r,t) - rB\frac{\partial C(r,t)}{\partial r} \tag{10}$$

where, A and B are constants which are functions of the rate constants of sequence alterations. The solution of the equation (10) is given by, $C(r,t) \sim \nu(t)r^{-\gamma}$; with $\nu \sim e^{\kappa t}$, where κ is a constant. The stationary ($t \to 0$) long range $C(r)$ follows power law as we have observed in the *HPR* and *SNP based sequences* (Figs 1, 2, 6 and 7) with $\gamma \to \theta_k$. Averaging the values of θ_ks of different isolate types in *HPR* and *SNP based sequences* (Fig. 6 Fourth and fifth column panels) respectively, we observe that in long range regime ($r \gg 1$):

- *HPR*: $C(r) \sim r^{-1/4}$; follows 1/4 scaling rule.
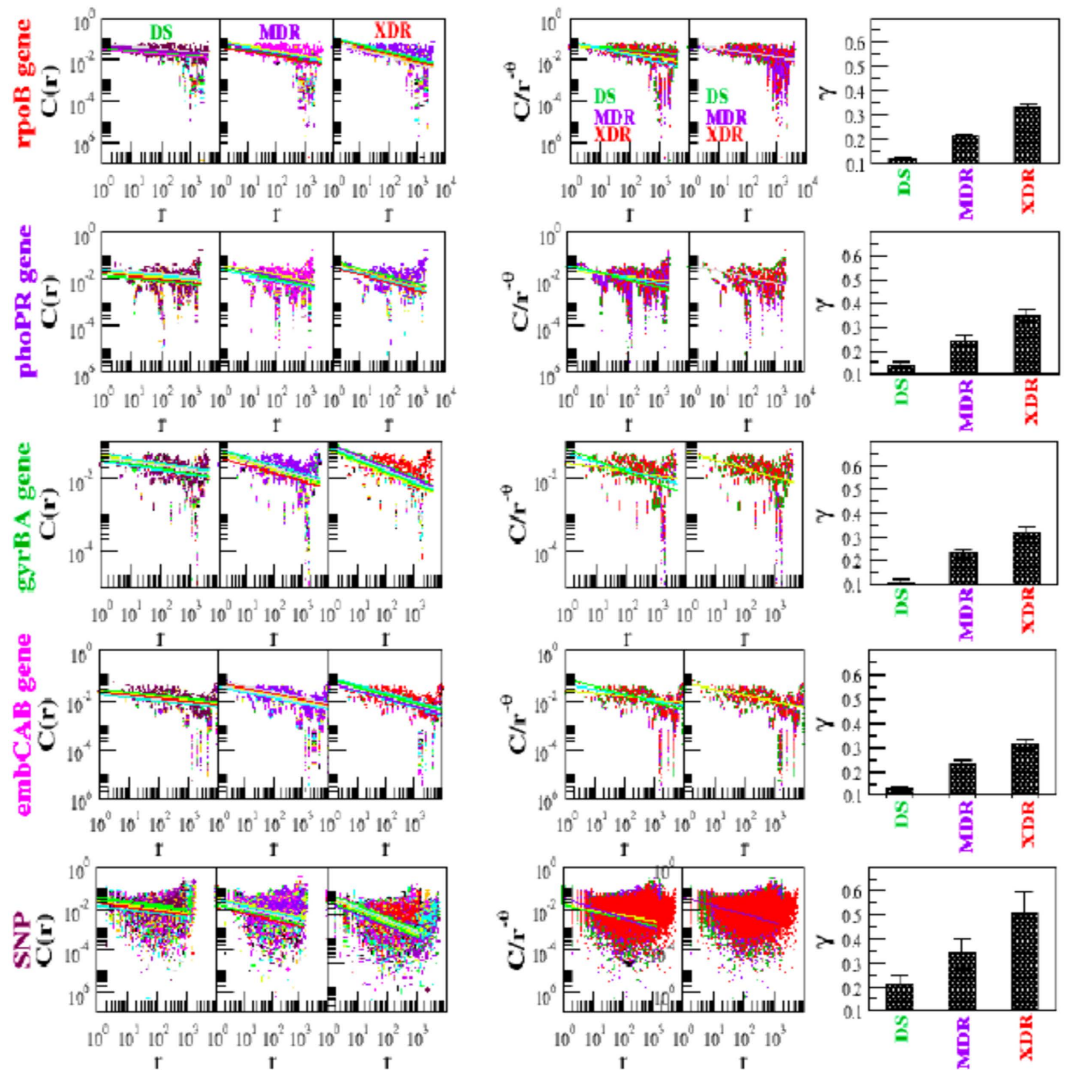- *SNP based sequences*: $C(r) \sim r^{-1/3}$; obeys 1/3 scaling law.

Figure 6. One parameter scaling law in correlation function of *rpoB* gene and SNP based sequences of DS, MDR and XDR of *M. tuberculosis*. (**a**) Scaling in *rpoB* gene for twenty isolates each of DS, MDR and XDR (panels of first row). The straight lines are power law fits to each isolate. The power law exponent (γ) for DS, MDR and XDR are given in rightmost panel of second row. The scaled data using Mackinnon and Kramer's one parameter scaling procedure[4] ($C(r)/r^{-\theta}$ as a function of r, see Methods) is shown in first two panels of second row. (**b**) Same scaling procedure is done for SNP based sequences (panels of third and fourth row).

However, in short range regime ($r \ll 1$) the nucleotides in the sequence follow Markov process[7,55], and therefore $C(r)$ decays with distance r of the nucleotide distribution, $C(r) \sim C_0 e^{-r/r_0}$, where, r_0 is the characteristics length scale.

The scaling behavior of the *HPR* can be studied by fitting the $C(r)$ data of *HPR* of each isolate with equation (9) and analyzing the scaling nature. The fitted lines on the data of DS type (forty isolates) are approximately parallel (Fig. 6 extreme left panel of first row). These data can then be scaled together by using one parameter scaling procedure[4,56] (see Methods) obeying $\theta_s \sim 0.13$ behavior (Fig. 6 fourth and fifth column panels). Applying the same one parameter scaling procedure, data of MDR and XDR isolates can also be scaled obeying $\theta_m \sim 0.23$ and $\theta_x \sim 0.33$ scaling rules respectively (Fig. 6 second, third and fourth column panels). These scaled data of DS, MDR and XDR can then be scaled together (Fig. 6 fourth and fifth column panels) following $\theta \sim 1/4$ scaling rule.

The same one parameter scaling procedure can also be done to the *SNP based sequence* data of DS, MDR and XDR isolates (Fig. 6 third and fourth rows). The scaled data follows $\theta \sim 1/3$ scaling law.

The scaling function Γ can be calculated in this regime using equation (1),

$$\lim_{r \to \infty} \Gamma[C(r)] = -\gamma v(t) \tag{11}$$

For short range correlated sequences (generated through Markov process), $C(r) \sim E e^{-\varepsilon r}$[48], and the scaling function can be obtained by,
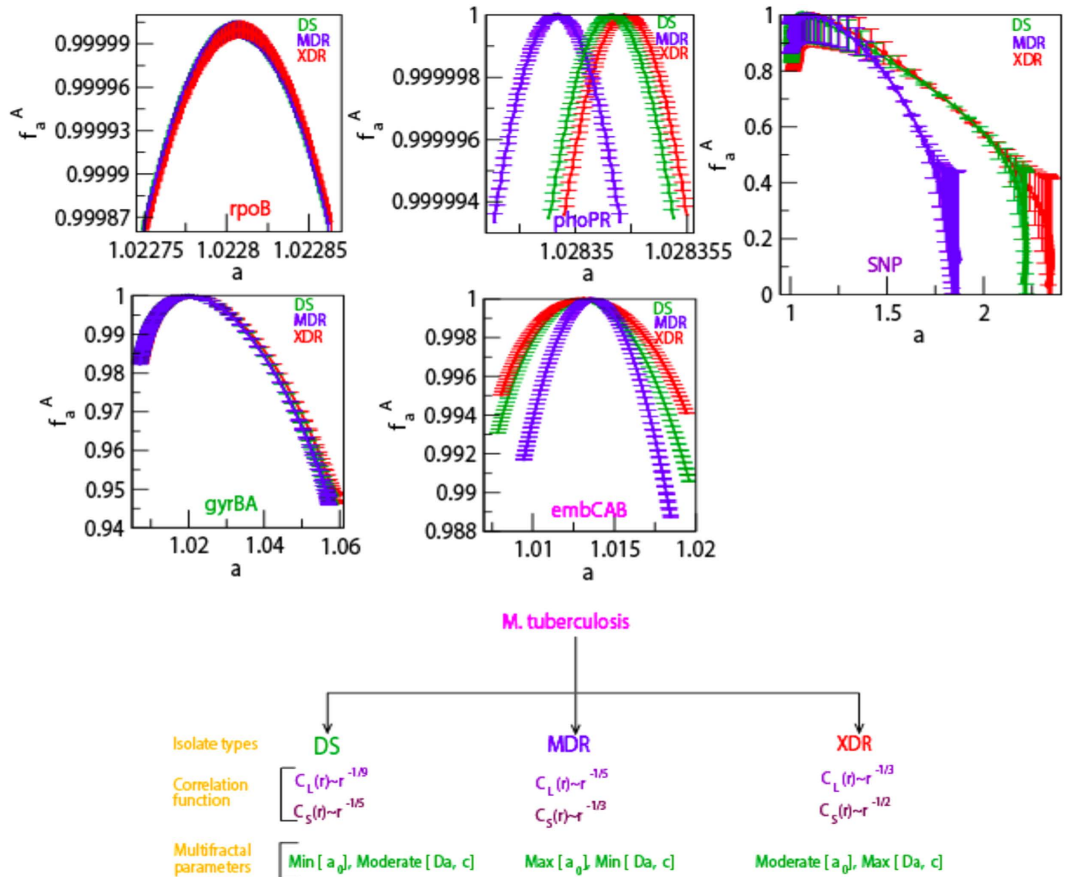
Figure 7. Multifractal and correlation function based classification of DS, MDR and XDR. The average singularity spectra of DS, MDR and XDR of *rpoB*, *phoPR*, *gyrBA*, *embCAB* and SNP based sequences (lower panel) as a function of α. The classification of DS, MDR and XDR based on Multifractal parameters and correlation function behaviors.

$$\lim_{r \to 0} \Gamma[C(r)] = \ln\left[\frac{C(r)}{E}\right]f \tag{12}$$

The obeying of one parameter scaling law in NGS genome indicates the signature of self-organization in the system.

Classification of *M. tuberculosis* isolates. Different isolates(DS, MDR and XDR) can be classified based on the multifractal and correlation properties found in the corresponding *HPR* and *SNP based sequences* (Figs 3, 4, 5, 6 and 7). The average values of singularity spectral parameters of these isolates (Fig. 7) show significant differences: 1. For α_0 ($f(\alpha_0) \to constant$) $\alpha_0^{DS} < \alpha_0^{XDR} < \alpha_0^{MDR}$; 2. For $\Delta\alpha$ (measure of multifractal complexity) $\Delta\alpha^{MDR} < \Delta\alpha^{DS} < \Delta\alpha^{XDR}$, and 3. For χ (measure richness in multifractality) $\chi^{MDR} < \chi^{DS} < \chi^{XDR}$. The nature of long range correlation function C(*r*) of these isolate types also exhibit significant behaviors (Fig. 7) as follows,

- For DS: correlation function in *HPR* follows, $C(r) \sim r^{-1/9}$ rule; and in *SNP based sequences* obeys $C(r) \sim r^{-1/5}$.
- For MDR: correlation function in *HPR* follows, $C(r) \sim r^{-1/5}$ rule; and in *SNP based sequences* obeys $C(r) \sim r^{-1/3}$.
- For XDR: correlation function in *HPR* follows, $C(r) \sim r^{-1/3}$ rule; and in *SNP based sequences* obeys $C(r) \sim r^{-1/2}$.

The behaviors of Multifractal parameters in DS, MDR and XDR of *M. tuberculosis* are found to distinctly different given by:

- For DS: *HPR* and SNP : $Min[\alpha_0]$, $Moderate[\Delta\alpha, \chi]$.
- For MDR: *HPR* and SNP : $Max[\alpha_0]$, $Min[\Delta\alpha, \chi]$.
- For XDR: *HPR* and SNP : $Moderate[\alpha_0]$, $Max[\Delta\alpha, \chi]$.
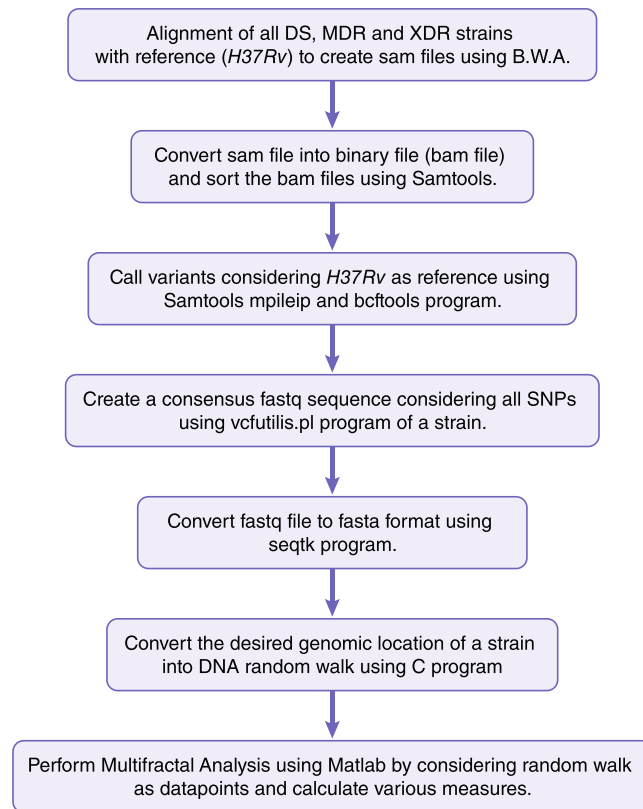
Figure 8. Computational Pipeline for Multifractal Analysis in *M. tuberculosis* bacterium.

We classified the NGS sequences of *M. tuberculosis* based on these two distinct properties of Multifractal parameters and correlation function (Fig. 7).

Conclusion

The genome evolution in *M. tuberculosis* involves alteration of nucleotides in different isolates of DS, MDR and XDR. It is important to remember that genomic alterations continuously takes place and drugs tend to target isolates with appropriate sequence. Normally there are insignificant changes in most of the genome involved in house keeping function needed for the organism to survive and grow[52]. The significant alterations of nucleotides in the genomes of various isolates take place in few regions of the genomes called HPR (hotspots and concatenated genes)[23–30,34,37]. Few of these conserved properties are multifractal nature and correlation function which are being inherited by these isolates from the parent genome with modified rules.

The multifractal nature in the *HPR* of the different *M. tuberculosis* isolates are due to long range correlations with small and large fluctuations, and significant probability distributions in the genome. The singularity spectra of these *HPR* of the isolates is able to capture small range of multifractality from singularity spectral parameters leading to slightly ordered state, but far from monofractality.

The scenario of multifractal properties is quite different in *SNP based sequences* of these isolates which can provide overall properties of the modified genome. These *SNP based sequences* show rich and complex multifractal nature characterized by fine structures in the sequences. This rich multifractal nature in *SNP based sequences* shows the perturbation in the reference genome, with these modified rules (multifractal and correlation nature) within the multifractal boundary for a change for fit survival.

The long range correlation function of *HPR* and *SNP based sequences* of these isolates follow 1/4 and 1/3 scaling rules respectively. The rules in the correlation function may be different in these isolates, but this property is inherited during evolution. Further, the correlation functions in different isolates follow one parameter scaling law indicating that it is one of the properties which keeps genome integrity.

Methods

DNA walk of *M. tuberculosis* NGS data.   The reads of the isolates of *M. tuberculosis* are downloaded from the Sequence Read Archive (SRA)[35,36]. Total 120 isolates are considered for our analysis. Forty isolates each from Drug sensitive (DS), Multi Drug Resitant (MDR) and Extremely Drug Resistant isolates (XDR) are considered. The reads are intially mapped to the reference genome *H37Rv* using BWA (Fig. 8)[57]. The BAM file is sorted using samtools and indexing of sorted bam file is performed[58]. In order to create a consensus sequence from the isolates the output of *samtools mpileup* is piped into *bcftools view* command, which in turn is piped into *vcfutilis.pl* program and finally a fastq file is created for the respective isolate. The fastq file is then converted into fasta file using *seqtk* program.

The fasta file is converted in *DNA walk* {x_i; $i = 1, 2, ..., N$} by considering purine (A and G) as step up ($x_i = +1$) and pyrimidine (C and T) as step down ($x_i = -1$)[38]. The *DNA walk* is considered to be a non stationary time series data due to its stochastic behavior which in turn can be used for various properties using Multifractal Detrened Fluctuation Average (MFDFA) analysis using Matlab program[59–61]. The detail procedure is shown in a flowchart below[8].

Multifractal DFA approach.

Multifractal detrended fluctuation analysis (MF-DFA) is a powerful technique to study fractal properties in nonstationary time series, and associated important correlations charactering the system[39]. Various important parameters which characterize the fractal nature of the time series and related properties, namely, Hurst exponent (*H*), generalized dimension (*D*), singularity spectrum (*f*) etc can be calculated numerically using a method adopted by Kantelhardt *et al.*[12] as summerized below. Firstly, the time series signal {x_j} of length *N* is taken as random walk, and can be represented by the profile, $Y(i) = \sum_{j=1}^{i}(x_j - \langle x \rangle)$, where, $\langle x \rangle$ is mean value of the signal, and $i = 1, 2, ..., N$. Second, the profile $Y(i)$ is now divided into $N_s = int\left(\frac{N}{s}\right)$ equal nonoverlapping equal segments of size *s*. To take into account all data points, $2N_s$ segments are considered by counting starting from both ends of the data. Third, the following variance is determined,

$$F^2(s, \nu) = \frac{1}{s}\sum_{i=1}^{s}\{Y[(\nu - 1)s + i] - y_\nu(i)\}^2 \tag{13}$$

where, $\nu = N_s + 1, ..., 2N_s$, and $y_\nu(i)$ is the fitting polynomial in segment ν. Fourth, the qth order fluctuation function is estimated by averaging over all segments,

$$F_q(s) = \left\{\frac{1}{2N_s}\sum_{\nu=1}^{2N_s}[Y[(\nu, s)]^{q/2}]\right\}^{1/q} \tag{14}$$

Fifth, the scaling behavior of the function $F_q(s)$ is represented by,

$$F_q(s) \sim s^{H_q} \tag{15}$$

where, H_q is the generalized Hurst exponent, which represents the measure of self-similarity and correlation properties of the signal. Then, H_q is related to classical scaling exponent $\tau(q)$ as,

$$\tau(q) = qH_q - 1 \tag{16}$$

and from the definition of Holder exponent, $\alpha = \frac{d\tau}{dq}$, the singularity function $f(\alpha)$[39] is given by,

$$f(\alpha) = q\alpha - \tau(q) \tag{17}$$

Then, generalized fractal dimension of the signal is measured by,

$$D_q = \frac{\tau(q)}{q - 1} \tag{18}$$

Now, D_0, for $q = 0$, is the fractal or Hausdorff dimension, D_1 is information dimension and D_2 represents correlation dimension[39]. Multifractal signature in the time series can be observed in the system if there exists significant dependence of H_q on *q* in the time series due to different scaling nature of small and large fluctuations[12]. Positive dependence of H_q on *q* indicates the scaling behavior of the time series segments with large fluctuations, whereas negative dependence of H_q on *q* exhibits scaling behavior in the time series segments with small fluctuations. Further, in multifractal time series, small and large fluctuations are characterized by large and small values of H_q.

Procedure for generating correlation function data.

Correlation function $C(r)$ of one dimensional genomic sequence {x_i; $i = 1, 2, ..., N$} of length *N* can be calculated following Messer *et al.* procedure[7] defined by,

$$C(r) = \sum_{k}^{N}\sum_{m \in \{A,C,G,T\}}[P(x_k = x_{k+r}|x_k = m) - P(x_k = m)^2] \tag{19}$$

where, $P(x_k = m)$ is the probability of finding a base *m* at position *k* in the genomic sequence, and $P(x_k = x_{k+r}|x_k = m)$ is the conditional probability to find the same base *m* at a distance *r* from *k*.

One parameter scaling law in correlation function.

The calculated correlation function C(r) of *HPR* of different isolates of NGS data of *M. tuberculosis*, where significant variation of sequences take place (hotspots and genes), follow power law behavior with approximately parallel fitted lines on *HPR* of different isolates (Fig. 2). This power law fitting on the data is verified and confirmed by following the fitting procedure proposed by Clauset *et al.*[62], where the value of *p* (statistical significant level) of each fitting is found to be larger than 0.1 which is the critical value of verifying that each data follow power law. We then follow one parameter scaling theory[3,4,56] to scale the data given by

$$\frac{C(r)}{r^{\theta}} = F\left[\frac{\xi}{r^{\theta}}\right], \tag{20}$$

where F is a scaling function. The form of the scaling function F and values of scaling exponent θ for DS, MDR and XDR isolates can be obtained by scaling the data of these isolates by fitting on the scaled data. Following this scaling procedure, and with the choice of ξ, we found that $F \rightarrow constant$ and obtained the following scaling law:

$$C(r) \propto r^{\theta}, \tag{21}$$

where $\theta = \{-\theta_s, -\theta_m, -\theta_x\}$ for HPR and SNP based sequence of different isolates of DS, MDR and XDR respectively.

Datasets. NGS datasets were downloaded from European Nucleotide Archive(ENA), EMBL. In Supplementary file Accession numbers and isolate Names are mentioned. Some SNP sequences were downloaded from Genome-based Mycobacterium Tuberculosis Variation (GMTV) Database.

References

1. Kadanoff, L. P. Scaling laws for Ising models near T_c. *Phys.* **2,** 263–272 (1966).
2. West, G. B. & Brown, J. H. Life's universal scaling laws. *Phys. Today* **57,** 36–42 (2004).
3. Abrahams, E., Anderson, P. W., Licciardello, D. C. & Ramakrishnan, T. V. Scaling Theory of Localization: Absence of Quantum Diffusion in Two Dimensions. *Phys. Rev. Lett.* **42,** 673 (1979).
4. Mackinnon, A. & Kramer, B. The scaling theory of electrons in disordered solids: additional numerical results. *Z. Phys. B.* **53,** 1–13 (1983).
5. Stoyan, D. & Mandelbrot, B. B. Fractals: Form, Chance, and Dimension. San Francisco. W. H. Freeman and Company. 1977. 352 S., 68 Abb., $14.95. *ZAMM Journal of Applied Mathematics and Mechanics/Zeitschrift fr Angewandte Mathematik und Mechanik* **59,** 402–403 (1979).
6. Calvert, L., Fisher, A. & Mandelbrot, B. The Multifractal Model of Asset Returns. *Discussion papers of the Cowles Foundation for Economics. Yale University: Cowles Foundation* **114–1166,** 12–27 (1997).
7. Messer, P. W., Arndt, P. F. & Lassig, M. Solvable sequence evolution models and genomic correlations. *Phys. Rev. Lett.* **94,** 138103 (2005).
8. Savage *et al. Func. Ecol.* **18,** 257 (2004).
9. West, G. B., Woodroff, W. H. & Brown, J. H. *Proc. Natl. Acad. Sci. USA* **99,** 2473 (2002).
10. Gates, M. A. A simple way to look at DNA. *Journal of Theoretical Biology* **119,** 319–328 (1986).
11. Liaofu, L. & Lu, T. Fractal dimension of nucleic acid sequences and the relation to evolutionary level. *Chin. Phys. Lett.* **5,** 421–423 (1988).
12. Kantelhardt, Jan W. *et al.* Multifractal detrended fluctuation analysis of nonstationary time series. *Physica A: Statistical Mechanics and its Applications* **316,** 87–114 (2002).
13. Movahed, M. S., Jafari, G. R., Ghasemi, F., Rahvar, S. & Tavar, M. R. R. Multifractal detrended fluctuation analysis of sunspot time series. *Journal of Statistical Mechanics: Theory and Experiment* **02** (2006).
14. Darko, S., Dusan, S., Tatijana, S. & Stanley, H. E. Multifractal analysis of managed and independent float exchange rates. *Physica A* **428,** 13–18 (2015).
15. Flores-Marquez, E. L., Ramirez-Rojas, A. & Telesca, L. Multifractal detrended fluctuation analysis of earthquake magnitude series of Mexican South Pacific Region. *Appl. Math. Compt.* **265,** 1106–1114 (2015).
16. Rotundo, G., Ausloos, M., Herteliu, C. & Ileanu, B. Hurst exponent of very long birth time series in XX century Romania, Social and religious aspects. *Physica A* **429,** 109–117 (2015).
17. Yin, Y. & Shang, P. Multiscale multifractal detrended cross-correlation analysis of traffic flow. *Nonlinear Dyn.* **81,** 1329–1347 (2015).
18. Yang, L., Zhu, Y. & Wang, Y. Multifractal characterization of energy stocks in China: a multifractal detrended fluctuation analysis. *Physica A* **451,** 357–365 (2016).
19. Maity, A. K., Pratihar, R., Mitra, A., Dey, S., Agrawal, V., Sanyal, S., Banerjee, A., Sengupta, R. & Ghosh, D. Multifractal detrended fluctuation analysis of alpha and theta EEG rhythms with musical stimuli. *Chaos, Solitons and Fractals* **81,** 52–67 (2015).
20. Moreno, P. A., Patricia, E. V., Ember, M., Luis, E. G., Daz, N., Siler, A., Irene, T., Jos, M. G., Ashwinikumar, K. N., Tobar, F. & Felipe, G. The human genome: a multifractal analysis. *BMC Genomics* **12,** 506 (2011).
21. Cole, STea *et al.* Deciphering the biology of Mycobacterium tuberculosis from the complete genome sequence. *Nature* **393,** 537–544 (1998).
22. World Health Organization. *Global Tuberculosis Report 2015, 20th edition* (2015).
23. Telenti, Amalio *et al.* Detection of rifampicin-resistance mutations in Mycobacterium tuberculosis. *The Lancet* **341,** 647–651 (1993).
24. Telenti, Amalio *et al.* Direct, automated detection of rifampin-resistant Mycobacterium tuberculosis by polymerase chain reaction and single-strand conformation polymorphism analysis. *Antimicrobial Agents and Chemotherapy* **37,** 2054–2058 (1993).
25. Banerjee, Asesh *et al.* inhA, a gene encoding a target for isoniazid and ethionamide in Mycobacterium tuberculosis. *Science* **263,** 227–230 (1994).
26. Zhang, Ying *et al.* The catalase-peroxidase gene and isoniazid resistance of Mycobacterium tuberculosis. *Nature* **358,** 591–593 (1992).
27. Takiff, Howard E. *et al.* Cloning and nucleotide sequence of Mycobacterium tuberculosis gyrA and gyrB genes and detection of quinolone resistance mutations. *Antimicrobial agents and chemotherapy* **38,** 773–780 (1994).
28. Sherman, David R. *et al.* Compensatory ahpC gene expression in isoniazid-resistant Mycobacterium tuberculosis. *Science* **272,** 1641–1643 (1996).
29. Telenti, A., Philipp, W. J., Sreevatsan S. *et al.* The emb operon, a gene cluster of Mycobacterium tuberculosis involved in resistance to ethambutol. *Nat Med* **3,** 567–70 (1997).
30. Scorpio, A. & Zhang, Y. Mutations in pncA, a gene encoding pyrazinamidase/nicotinamidase, cause resistance to the antituberculous drug pyrazinamide in tubercle bacillus. *Nat Med* **2,** 662–7 (1996).
31. Comas, I. *et al.* Human T cell epitopes of Mycobacterium tuberculosis are evolutionarily hyperconserved. *Nat Genet* **42,** 498–503 (2010).
32. Feuk, L., Carson, A. R. & Scherer, S. W. Structural variation in the human genome. *Nature Reviews Genetics* **7,** 85–97 (2006).
33. Koutras, M. V., Bersimis, S. & Maravelakis, P. E. Statistical Process Control using Shewhart Control Charts with Supplementary Runs Rules. *Methodology and Computing in Applied Probability* **9,** 207–224 (2007).
34. Walters, Shaun B. *et al.* The Mycobacterium tuberculosis PhoPR two component system regulates genes essential for virulence and complex lipid biosynthesis. *Molecular microbiology* **60,** 312–330 (2006).
35. Leinonen Rasko, Hideaki Sugawara & Martin Shumway. The sequence read archive. *Nucleic acids research* gkq1019 (2010).

36. Chernyaeva, Ekaterina N. *et al.* Genome-wide Mycobacterium tuberculosis variation (GMTV) database: a new tool for integrating sequence variations and epidemiology. *BMC genomics* **15,** 308 (2014).
37. Das, Sarbashis *et al.* Identification of Hot and Cold spots in genome of Mycobacterium tuberculosis using Shewhart Control Charts. *Scientific reports* **2** (2012).
38. Peng, C. K., Buldyrev, S. V., Goldberger, A. L., Havlin, S., Sciortino, F., Simons, M. & Stanley, H. E. Long-range correlations in nucleotide sequences. *Nature* **356,** 168–170 (1992).
39. Halsey, Thomas C. *et al.* Fractal measures and their singularities: the characterization of strange sets. *Physical Review A* **33,** 1141 (1986).
40. Mallat, S. & Hwang, W. L. Singularity detection and processing with wavelets. *IEEE Trans. Infor. Theor.* **28,** 617 (1992).
41. Hentschel, H. & Procaccia, I. *Physica D* **8,** 435–444 (1983).
42. Grassberger, P. *Phys. Lett. A* **97,** 227–230 (1983).
43. Feder, J. *Fractals*, Plenum Press, New York 9 (1988).
44. Peitgen, H.-O., Jurgens, H. & Saupe, D. *Chaos and Fractals*, Springer, New York (1992).
45. Kantelhardt, J. W., Eva, K.-B., Rybski, D., Braum, P. Bunde, A. & Havlin, S. Long-term persistence and multifractality of precipitation and river runoff records. *J. Geophys. Res.* **111,** D01106 (2006).
46. Norouzzadeh, P. & Rahmani. *Physica A* **367,** 328 (2006).
47. Shimizu, Y., Thurner, S. & Ehrenberger, K. Multifractal spectra as a measure of complexity in human posture. *Fractals* **10,** 103 (2002).
48. Messer, P. W., Bundschuh, Vingron, M. & Arndt, P. F. Effects of Long-Range Correlations in DNA on Sequence Alignment Score Statistics. *J. Compt. Biol.* **14,** 655–668 (2007).
49. Clauset, A. *et al.* Power-law distributions in empirical data. *SIAM Rev. Soc. Ind. Appl. Math.* **51,** 661–703 (2009).
50. Gandhi, N. R., Paul, N., Keertan, D., Schaaf, H. S., Matteo, Z., Soolingen, D. V., Jensen, P. & Bayona, J. *Lancet* **375,** 1830–1843 (2010).
51. Holland, John H. & Hidden, H. Order: how adaptation builds complexity. *Basics Book* (1996).
52. Heylighen, F. The science of self-organization and adaptivity. *The encyclopedia of life support systems* **5,** 253–280 (2001).
53. Frieden, T. R., Sterling, T., Ariel, P.-M., Kilburn, J., Cauthen, G. M. & Dooley, S. W. The emergence of drug-resistant tuberculosis in New York city. *New England J. Med.* **328,** 521–526 (1993).
54. Saakian, D. B. Evolution models with base substitutions, insertions, deletions and selection. *Phys. Rev. E* **78,** 061920 (2008).
55. Bernaola-Galvan, P., Carpena, P., Roman-Roldan, R. & Oliver, J. L. *Gene* **300,** 105–115 (2002).
56. Pichard, J. L. & Sarma, G. Finite size scaling approach to Anderson localisation. *J. Phys. C* **14,** L127–L132 (1981).
57. Li, H. & Durbin, R. Fast and accurate short read alignment with Burrows-Wheeler transform. *Bioinformatics* **25,** 1754–1760 (2009).
58. Li, Heng *et al.* The sequence alignment/map format and SAMtools. *Bioinformatics* **25,** 2078–2079 (2009).
59. Gu, Gao-Feng & Wei-Xing, Zhou. Detrending moving average algorithm for multifractals. *Physical Review E* **82,** 011136 (2010).
60. Ihlen, Espen A. F. Introduction to multifractal detrended fluctuation analysis in Matlab. *Fractal Analyses: Statistical And Methodological Innovations And Best Practices* **97** (2012).
61. Xu, Limei *et al.* Quantifying signals with power-law correlations: A comparative study of detrended fluctuation analysis and detrended moving average techniques. *Physical Review E* **71,** 051101 (2005).
62. Clauset, A., Shalizi, C. R. & Newman, M. E. J. Power-law distributions in empirical data. *SIAM Rev. Soc. Ind. Appl. Math.* **51,** 661–703 (2009).

Acknowledgements

Author Contributions

S.M. and R.K.B.S. conceived the model. S.M. did the numerical experiment and prepared the figures of the numerical results. R.K.B.S. and S.M. analyzed and interpreted the simulation results, and wrote the manuscript. T.R.C. generated *SNP* data. S.M., T.R.C., K.C., A.B., and R.K.B.S. are involved in the study, reviewed and approved the manuscript.

Additional Information

Supplementary information accompanies this paper at http://www.nature.com/srep

Competing Interests: The authors declare no competing financial interests.

How to cite this article: Mandal, S. *et al.* Complex multifractal nature in *Mycobacterium tuberculosis* genome. *Sci. Rep.* **7,** 46395; doi: 10.1038/srep46395 (2017).

Publisher's note: Springer Nature remains neutral with regard to jurisdictional claims in published maps and institutional affiliations.